Proceedings of the Sixth International Conference on
Railway Technology: Research, Development and Maintenance
Edited by: J. Pombo
Civil-Comp Conferences, Volume 7, Paper 16.11
Civil-Comp Press, Edinburgh, United Kingdom, 2024
ISSN: 2753-3239, doi: 10.4203/ccc.7.16.11

Research on the Characteristic of Ultra-High Speed Linear Motor

Y. Hu[1,2], G. Lin[1,2], Z. Long[3] and X. Ma[1,2]

[1]Key Laboratory of Railway Industry of Maglev Technology, Tongji University, Shanghai, China
[2]Maglev Transportation Engineering R&D Center, Tongji University, Shanghai, China
[3]College of Intelligence Science and Technology, National University of Defense Technology, Changsha, China

Abstract

Based on vector magnetic potential and scalar magnetic potential, the theoretical model of bilateral permanent magnet synchronous linear motor is established, and the analytical expression of the magnetic field in the target region is given. Based on the expression, the variation of magnetic field with wavelength, air gap and thickness of permanent magnetic material is analyzed, and the reasonable range of wavelength design value is pointed out. The formula of electromagnetic force is derived, and the expression of electromagnetic force produced by permanent magnetic material per unit weight is obtained.

Keywords: magnetic levitation train, permanent magnet, electromagnetic force, magnetic field, linear motor, magnetic potential

1 Introduction

With the demand of vacuum tube maglev traffic [1,2] and ground ultra-high speed test [3,4], the research of ultra-high speed linear motor has gradually become a research hotspot.

Ultra-high speed linear motor can use either linear induction motor or linear synchronous motor. The former has a relatively simple structure with a light mover, and has an advantage of low cost, low power factor and low efficiency under large air gap. The latter's power system is relatively complex with high cost with high power density, high power factor, efficiency and complex control. Considering the advantages of the permanent magnet synchronous linear motor, it is more suitable to achieve ultra-high-speed traction [5-7]. At present, experts have carried out a lot of research on the maglev technology in the field of super-high speed, but the permanent magnet synchronous linear motor traction technology still needs to be deeply studied. Based on the above statement, this paper takes the permanent magnet synchronous linear motor as the research object to study the characteristic of ultra-high speed maglev propulsion system.

2 Physical modelling

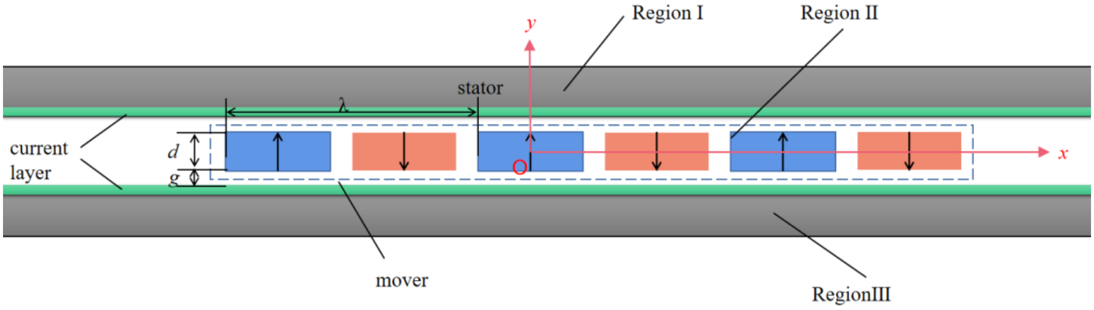

Figure 1: Structure diagram of bilateral permanent magnet synchronous linear motor

Considering the requirement of ultra-high speed for high thrust, this paper discusses the structure of bilateral long stator permanent magnet synchronous linear motor, as shown in Figure 1. The groove and winding area are defined as the current layer. It has the purpose of simplifying the physical model by reducing the number of solving domains in the spatial region. Make the following assumption:

(1) The iron core thickness is infinitely thick;

(2) The magnetic field does not change along the vertical paper surface;

(3) The permanent magnet material is high residual magnetic NdFeB, and the influence of permanent magnetic field on the space magnetic field is ignored;

(4) Ignore the end effect.

According to the principle of permanent magnet synchronous linear motor, the greater the horizontal component of the magnetic field is, the stronger the thrust of the electromagnet is. Therefore, in order to simplify the modeling, the electromagnetic field modeling after mover removal is considered. As shown in Figure 1, the solution region was classified as 3 solution domains. Domain I and III are the eddy current field domain, both of the electromagnetic field distribution with respect to the x-axis are symmetrical. The remaining area is air domain. Assuming the air gap length is g, the permanent magnet thickness is d and the wavelength is λ. For region II, this paper focuses on the magnitude of the horizontal component of the magnetic field direction, especially at $y=d/2$. Typically, vector magnetic potential are used for the region containing the free current. Both scalar magnetic potential and vector magnetic potential can be used for the air domain without free current, and the two are equivalent.

2.1 Governing equations

For region I, a vector magnetic potential description may be used by:

$$A_z^{\mathrm{I}}(x,y,t)=\mathrm{Re}\left\{\dot{A}_z^{\mathrm{I}}(y)e^{\mathrm{j}(kx-\omega t)}\right\} \tag{1}$$

Note that the vector magnetic potentials of the 2D model have only the *z*-axis component in region I and III, and the vector magnetic potentials of region III are described similarly to the region I, and will not be described here. In the above equation, j is the imaginary unit, and $k=2\pi/\lambda$. If the traveling wave magnetic field velocity is v, then $\omega=kv$ holds in the above equation.

For scalar magnetic potential description:

$$\varphi^{\mathrm{II}}(x,y,t)=\mathrm{Re}\left\{\dot{\varphi}^{\mathrm{II}}(y)e^{\mathrm{j}(kx-\omega t)}\right\} \tag{2}$$

Then the electromagnetic field governing equations of regions I and II are respectively

$$\left(\frac{\partial^2}{\partial x^2}+\frac{\partial^2}{\partial y^2}-\mu\sigma\frac{\partial}{\partial t}\right)A_z^{\mathrm{I}}(x,y,t)=0 \tag{3}$$

$$\left(\frac{\partial^2}{\partial x^2}+\frac{\partial^2}{\partial y^2}\right)\varphi^{\mathrm{II}}(x,y,t)=0 \tag{4}$$

2.2 Boundary condition

To simplify the solution, suppose the core thickness is sufficiently large, i. e

$$A_z^{\mathrm{I}}(x,+\infty,t)=0 \tag{5}$$

At the junction of regions I and region II, it holds

$$-\frac{\partial A_z^{\mathrm{I}}(x,d/2+g,t)}{\partial x}=-\mu_0\frac{\partial\varphi^{\mathrm{II}}(x,d/2+g,t)}{\partial y} \tag{6}$$

Assuming that the current density of the stator winding along the *x*-direction is $I=\dot{I}\mathrm{e}^{\mathrm{j}(kx-\omega t)}$, then

$$-\frac{1}{\mu}\frac{\partial A_z^{\mathrm{I}}(x,d/2+g,t)}{\partial y}-\mu_0\frac{\partial\varphi^{\mathrm{II}}(x,d/2+g,t)}{\partial x}=I \tag{7}$$

Moreover, considering the symmetry, region III is no longer solved. A symmetry condition needs complemented

$$\frac{\partial\varphi^{\mathrm{II}}(x,0,t)}{\partial x}=0 \tag{8}$$

2.3 Solutions of electromagnetic fields

According to formula (1) ~ (8), the horizontal component of the magnetic field in the region II is

$$\begin{aligned}H_x^{\mathrm{II}}(x,y,t)&=-\frac{\partial\varphi^{\mathrm{II}}(x,y,t)}{\partial x}\\&=\mathrm{Re}\left\{-\frac{k\dot{I}(\mathrm{e}^{ky}-\mathrm{e}^{-ky})}{k(\mathrm{e}^{k(g+d/2)}-\mathrm{e}^{-k(g+d/2)})+q\mu_0/\mu(\mathrm{e}^{k(g+d/2)}+\mathrm{e}^{-k(g+d/2)})}\mathrm{e}^{\mathrm{j}(kx-\omega t)}\right\}\end{aligned} \tag{9}$$

In the above equation, $q=\sqrt{k^2-i\mu\sigma kv}$. Considering the infinite permeability of the stator region, the above equation reduces to

$$H_x^{\mathrm{II}}(x,y,t)=\mathrm{Re}\left\{-\frac{\dot{I}(\mathrm{e}^{ky}-\mathrm{e}^{-ky})}{(\mathrm{e}^{k(g+d/2)}-\mathrm{e}^{-k(g+d/2)})}\mathrm{e}^{\mathrm{j}(kx-\omega t)}\right\} \tag{10}$$

Because the electromagnetic thrust is proportional to the horizontal direction component of the magnetic field in the region where the mover is located, it can be seen from the above equation that the electromagnetic thrust is proportional to the current of the stator winding. Based on the above results, the variation of the magnetic field in region II will be further explored.

3 Magnetic field analysis

Let $\beta(y)=\frac{(\mathrm{e}^{ky}-\mathrm{e}^{-ky})}{(\mathrm{e}^{k(g+d/2)}-\mathrm{e}^{-k(g+d/2)})}$, then $0<\beta<1$ and can represent the intensity of the target magnetic field. When $y=d/2$,

$$\beta=\frac{(\mathrm{e}^{kd/2}-\mathrm{e}^{-kd/2})}{(\mathrm{e}^{k(g+d/2)}-\mathrm{e}^{-k(g+d/2)})} \tag{11}$$

When the wavelength λ is 0.05m,0.1m,0.3m,0.5m,0.7m,0.9m, the permanent magnet thickness d is 50mm, and the air gap g is 5~10mm, the change of β is studied. As shown in Figure 2, the variable β generally decreases exponentially with the air gap, consistent with the actual situation that the magnetic field strength decreases with the air gap. When the wavelength is gradually increased, the variable β decreases more slowly. When the wavelength is greater than or equal to 0.5m, the loss is less than 0.1. When the wavelength is less than 0.3m, the loss of variable β with the air gap g is greater than 0.2. This means that when the wavelength is greater than 0.5m, the error of the design amount of the air gap will not cause a large change of the air gap magnetic field, so that the air gap design can tolerate a high error. Therefore, it is more reasonable to choose more than 0.5m in the wavelength design.

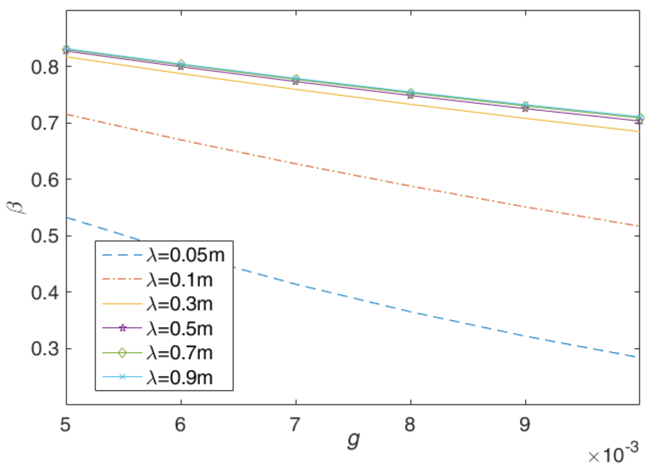

Figure 2: The variation of variable β with the air gap g when the thickness of the permanent magnet material is 50mm

In order to investigate the influence of the thickness of the permanent magnet on the strength of the magnetic field, to make the values of the wavelength and air gap consistent with the above; the thickness of the permanent magnet d adopts 40mm, 30mm and 20mm respectively. The change of β is as shown in Figure 3 to Figure 5. We can see that the change trend of β is not changed. The variable β also did not change significantly with the change law of the air gap.

The thickness of the permanent magnet has a significant influence on the variable β, and the thinner the permanent magnet is, the weaker the magnetic field is. Therefore, the larger the thickness of the permanent magnet, the better.

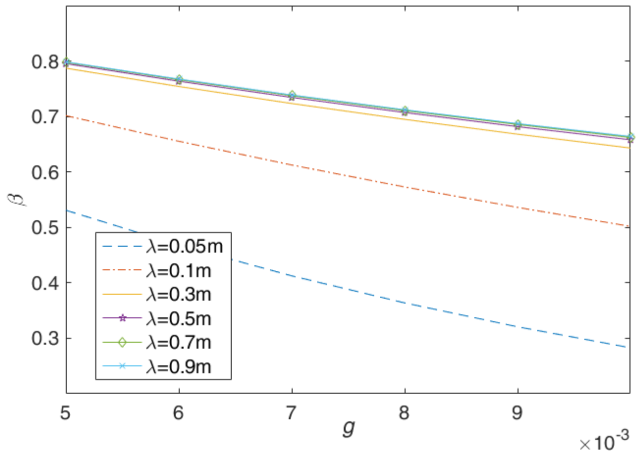

Figure 3: The variation of variable β with the air gap g when the thickness of the permanent magnet material is 40mm.

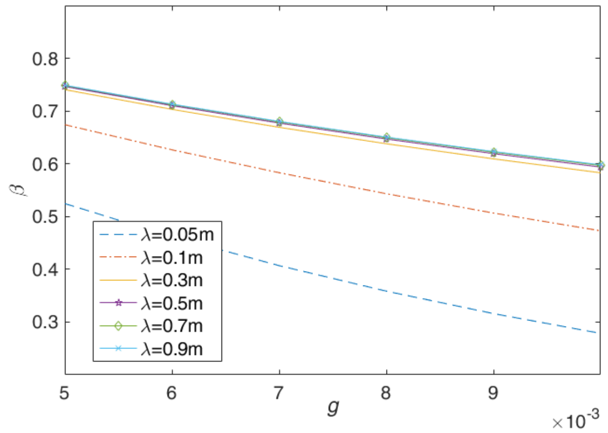

Fig ure 4: The variation of variable β with the air gap g when the thickness of the permanent magnet material is 30mm

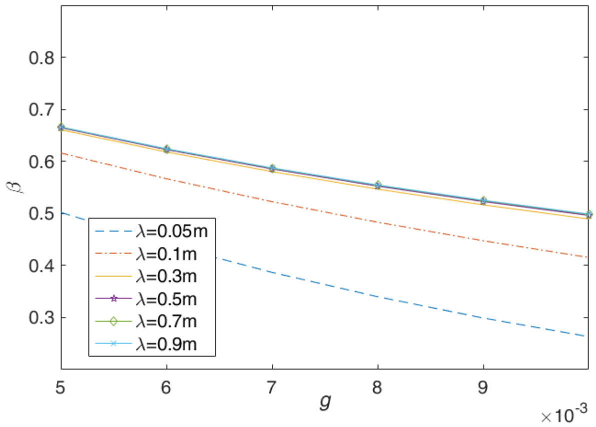

Figure 5: The variation of variable β with the air gap g when the thickness of the permanent magnet material is 20mm

4 Magnetic force analysis

The magnetic charge distribution along the x-axis is assumed as:

$$\sigma_{\mathrm{m}} = \mathrm{Re}\left\{-\dot{\sigma}_{\mathrm{m}} \mathrm{e}^{j(kx-\omega t)}\right\} \tag{12}$$

Then, the electromagnetic thrust line density expression of the permanent magnet synchronous linear motor is:

$$F_x = -2 \times \frac{1}{2} \sigma_m^* H_x^{\mathrm{II}}(x,y,t) = \dot{\sigma}_m \dot{I} \beta(d/2) \tag{13}$$

It can be seen that the electromagnetic thrust is proportional to $\beta(d/2)$, the total length of the permanent magnet is l, and the thickness is d, the ratio of the thrust to the weight of the permanent magnet is a dimensionless amount, which is expressed by

$$\begin{aligned} \gamma &= \frac{\dot{\sigma}_m \dot{I} l \beta(d/2)}{\rho l d g} \\ &= \frac{\dot{\sigma}_m \dot{I}}{\rho g} \frac{\beta(d/2)}{d} \\ &= \frac{\dot{\sigma}_m \dot{I}}{\rho g} \frac{(\mathrm{e}^{kd/2} - \mathrm{e}^{-kd/2})}{d(\mathrm{e}^{k(g+d/2)} - \mathrm{e}^{-k(g+d/2)})} \end{aligned} \tag{14}$$

Let $\eta = \frac{(\mathrm{e}^{kd/2} - \mathrm{e}^{-kd/2})}{d(\mathrm{e}^{k(g+d/2)} - \mathrm{e}^{-k(g+d/2)})}$, Then, it reflects the ratio of the thrust to the weight of the permanent magnet, and its change trend with the thickness of the permanent magnet is shown in Figure 6 to Figure 8. It can be seen that, η decrease rapidly with the increase of the air gap, which means that the permanent magnet material usage decreases significantly with the increase of the air gap. Therefore, it shows that η decrease rapidly with the permanent magnet thickness, indicating that the permanent magnet material usage decreases significantly with the increase of the magnet thickness.

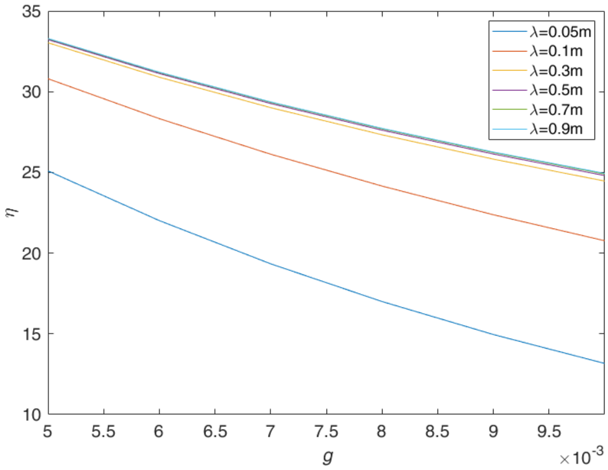

Figure 6: The variation of variable η with the air gap g when the thickness of the permanent magnet material is 20mm

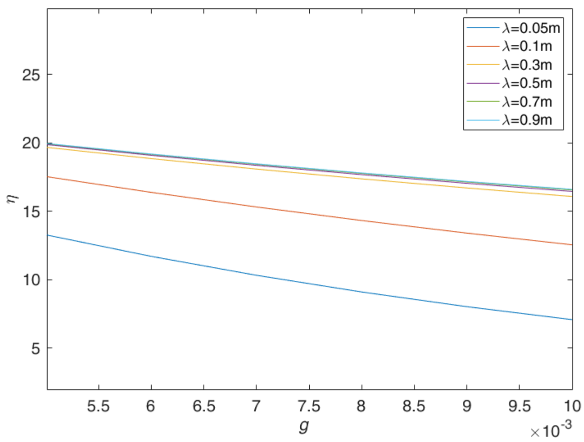

Figure 7: The variation of variable η with the air gap g when the thickness of the permanent magnet material is 40mm

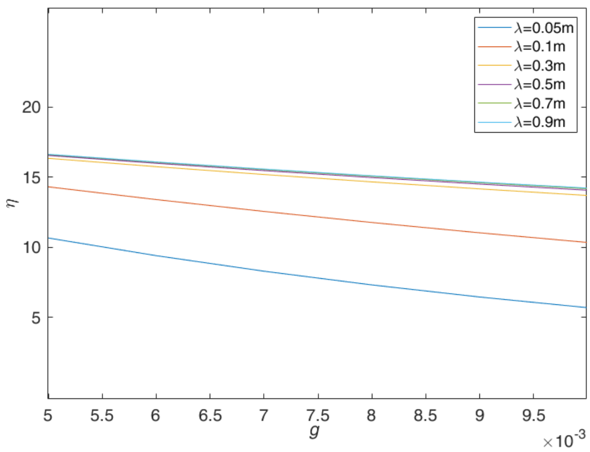

Figure 8: The variation of variable η with the air gap g when the thickness of the permanent magnet material is 50mm

Obviously, the usage of permanent magnet materials decreases with both the permanent magnet thickness and the air gap. Therefore, the gap design should not be too large; the thickness design of permanent magnet should be considered to meet with the actual demand of electromagnetic thrust.

5 Conclusions

By establishing the model of bilateral long stator permanent magnet synchronous linear motor, the electromagnetic characteristics and permanent magnet usage are studied. The main conclusions are as follows:

(1) Based on the scalar magnetic field and the vector magnetic field, the electromagnetic physics model of the permanent magnet synchronous linear motor is established, and the analytical expression of the electromagnetic field is obtained. The analysis results show that when the wavelength design should be more than 0.5m, and a large thickness of permanent magnet is beneficial to promote the electromagnetic thrust.

(2) The analytical expression of electromagnetic thrust is given. It is pointed out that the effective way to improve the usage of permanent magnet is to reduce the gap.

This paper ignores the nonlinear characteristics of the stator core, but the model could still be used for the preliminary design of ultra-high linear motor.

Acknowledgement

This work was supported in part by the National Natural Science Foundation of China under Grant 52332011, 52232013, 52072269 and 52372359.

References

[1] HU Xiao, MA Tianhao, WANG Xiaofei, et al. Scale effect of aerodynamic characteristics in evacuated tube maglev transport[J]. Journal of Southwest Jiaotong University, 2023, 58(4) : 808-819.

[2] J Y, LI T, ZHANG X H, et al. Research on aerodynamic and thermal characteristics of subsonic evacuated tube maglev system[J]. Acta Aerodynamica Sinica, 2022, 40(2): 115−121(in Chinese).

[3] Record of Decision for the United States Air Force Special Use Airspace Optimization at Holloman Air Force Base Environmental Impact Statement[J]. U.S. Department of Defense Information / FIND,2021,86(066).

[4] Flankl M , Wellerdieck T , Tuysuz A ,et al.Scaling laws for electrodynamic suspension in high-speed transportation[J]. IET Electric Power Applications, 2017, 12(3):357-364.

[5] LI Guanchun. Theoretical Study and Control Methods of Super High Speed and Large Thrust LinearMotor[D]. National University of Defense Technology,2020.

[6] CHEN Qiang. Research on Design and Control Technology of Super High Speed Suspension System[D]. National University of Defense Technology,2018.

[7] HU Yongpan, ZENG Jiewei, WANG Zhiqiang, et al. Performance optimization of ultra-high speed permanent magnet electrodynamic suspension system[J]. Journal of Southwest Jiaotong University, 2023， 58(4)： 773-782.